doi:10.3772/j.issn.1006-6748.2018.03.012

Stroke optimization of a novel multi-station rotary polishing robot based on workspace analysis①

Li Dongjing(李东京)②[*,**], Wei Wang[*], Wang Qilong[*], Hao Daxian[*], Jin Hui[***]
([*] School of Information and Electrical Engineering, Hubei University of Science and Technology, Xianning 437100, P. R. China)
([**] School of Mechanical Engineering and Automation, Beihang University, Beijing 100191, P. R. China)
([***] College of Mechanical Engineering, Chongqing University of Technology, Chongqing 400054, P. R. China)

Abstract

In order to meet the polishing requirement of faucets and other products, a novel multi-station rotary polishing robot is designed, which is a PPPR + RR type of degree of freedom (DOF) distribution structure, and is similar to dual-arm robot. Forward and inverse kinematic analysis is carried out by robot modeling. In order to make this robot structure more compact, first of all, X, Y and Z three moving degrees of freedom (DOF) limit stroke polishing need is calculated by using an artificial fish swarm algorithm, which analyzes dexterous workspace of this robot. Then, on the basis of the above analysis, the three DOF stroke is optimized. Simulation and polishing experimental results verify that this polishing robot with optimized stroke parameters can meet the polishing needs of faucets and other bathroom pieces.

Key words: multi-station rotary table polishing robot, dexterous workspace analysis, stroke optimization, dual-arm robot, artificial fish swarm algorithm (AFSA)

0 Introduction

Polishing is one of the most important finishing process forms for many products. But there are some problems in the polishing process such as bad working environment, easiness to produce dust and explosion risk. With the development of industrial automation, it is more and more difficult to meet the needs of production by using the traditional polishing form with manual or traditional machine tools. Therefore, it is necessary to design a polishing machine that can meet the needs of modern production. Nowadays robot is applied more and more widely including robot welding, robot handling, etc. Because of its high flexibility and large working space, and other remarkable advantages, robot machining has attracted more attentions and researches in the field of traditional machine tool processing. At present, robots have been applied in the fields of grinding, polishing and milling. Many scholars at home and abroad have done a lot of researches on robot machining[1-4]. Specific to polishing processing, universal series robot is used to handle workpiece to finish polishing currently on the market. But this single-piece production is inefficient. In order to improve the efficiency, a multi-station polishing machine that can polish some workpieces at same time is developed. Zhang[5,6] analyzed and studied layout optimization, flexible workspace analysis, force control and other aspects of this multi-station simultaneous polishing robot. Although this type of polishing robot improved efficiency, completing workpiece polishing requires several times installing, which reduced efficiency and increased machining error. At the same time, the consistency of the processing quality is not good enough. In order to solve these problems, a novel rotary table multi-station polishing robot is designed. To make the robot structure compact as much as possible while meeting the requirement of polishing workspace and dexterous workspace, it is necessary to optimize the structure of this polishing robot. For the robot structure design and parameter optimization, Many studies[7-10], such as genetic algorithm (GA), particle swarm algorithm (PSA), neural network (NN) and other intelligent algorithms have been mostly applied to optimize robot. The polishing robot designed is similar to the dual arm robot. There are also many research results on the optimization of the parameters of the robot and the layout of the dual arm robot[11-13]. Among many intelligent optimization algorithms, the artificial fish

① Supported by the Key Research and Development Project of Yangzhou——Industry Preview and Key Projects (No. YZ2015011).
② To whom correspondence should be addressed. E-mail: ltokyo@126.com
Received on Nov. 23, 2017

swarm algorithm has the advantages of global optimization, and has been widely studied and applied in recent years[14-26]. The artificial fish swarm algorithm is used to optimize the stroke of the polishing robot. The rest of the paper is organized as follows. Section 1 introduces the structure of the polishing robot. Section 2 analyze the kinematics of this robot. In Section 3, required limit stroke of various DOF of the polishing robot is analyzed by AFSA and the stroke is optimized based on dexterous workspace analysis. In Section 4 the machining experience confirms that the optimized stroke can meet the requirements of polishing, and at the end a summary of the research work is presented.

1 Structure of polishing robot

For bathroom parts such as faucets (Fig. 1), it has the characteristics of large batch and high appearance requirements. In order to improve the efficiency of faucets polishing and reduce the times of installing, a novel multi-station rotary table faucet polishing robot system is designed as shown in Fig. 2.

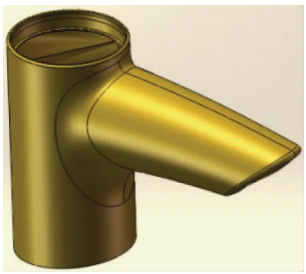

Fig. 1 The faucet to be polished processing

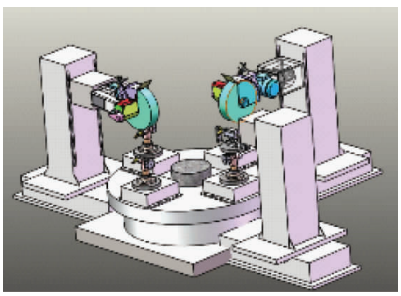

Fig. 2 The multi-station rotary table faucet polishing robot

As shown in Fig. 2, the center of the polishing robot is equipped with 4 tap mounting stations, 3 work stations among which 4 mounting stations are used to produce, and the remaining stations are the loading and unloading stations.

Three polishing robots are arranged outside the rotary table, which can be used to polish at the same time. The faucet polishing robot with this structure carries out polishing production in accordance with the following steps.

1) The faucet to be polished is mounted at the loading station.

2) The rough polishing robot corresponding to the faucet mounting station performs rough polishing of the faucet.

3) After the rough polishing, the rotary table rotates 90°, the faucet will be aimed at intermediate polishing robot station and to be polished intermediatly.

4) After that, the rotary table rotates 90°, the faucet after intermediate polishing will be aimed at finishing polishing robot station and to be finishing polished.

5) The rotary table rotates 90° and this faucet is polished fine. Remove it and mount another faucet to be continously processed.

The machining process is shown in Fig. 3.

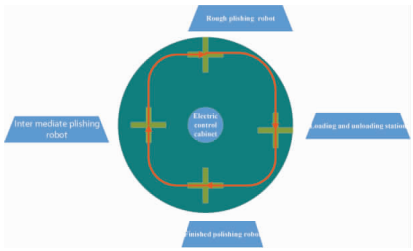

Fig. 3 The faucet polishing process

The DOF distribution of the polishing robot is shown in Fig. 4.

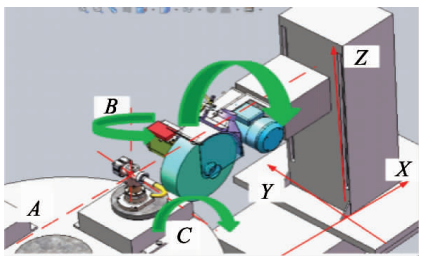

Fig. 4 The polishing robot DOF distribution

It can be seen that the DOF of the robot is distributed to two parts: the fixture on the middle rotary table has two rotation DOF of B and C; the surrounding polishing robot has four DOF of X, Y, Z and A. This PPPR + RR type DOF distribution is helpful to improve the working space of the polishing robot.

2 Kinematic analysis

2.1 Forward kinematics

The coordinate system of the polishing robot is established as shown in Fig. 5.

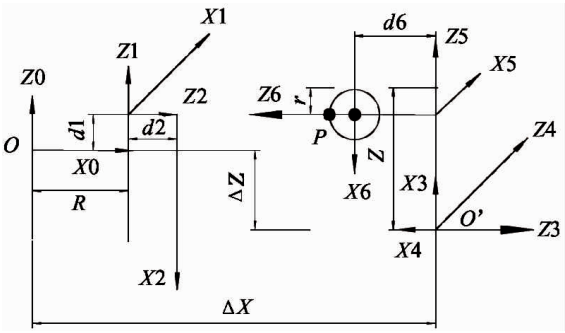

Fig. 5 The coordinate system

In Fig. 5, the fixture $\{O\}$ coordinate system D-H parameter is shown in Table 1.

Table1 Fixture $\{O\}$ coordinate system D-H

DOF	a_{i-1}	α_{i-1}	d_i	θ_i
0	R	0	0	0
1	0	90°	d_1 =210	θ_1
2	0	0	d_2	90° + θ_2

According to the D-H parameters of the fixture coordinate system, the conversion matrix of the fixture coordinate system is shown in Eq. (1).

$$\boldsymbol{T}_{02} = \boldsymbol{T}_{01}\boldsymbol{T}_{12} = \begin{bmatrix} -c_1c_2 & -c_1s_2 & s_1 & R + d_2s_1 \\ -c_2s_1 & -s_1s_2 & -c_1 & -d_2c_1 \\ c_2 & -s_2 & 0 & d_1 \\ 0 & 0 & 0 & 1 \end{bmatrix} \tag{1}$$

If the workpiece coordinate system is $\{W\}$, then $\{W\}$ relative to the $\{O\}$ coordinate system is

$$\boldsymbol{T}_{oW} = \boldsymbol{T}_{02}\boldsymbol{T}_{2W} \tag{2}$$

According to the *Z-Y-Z* Euler angle theorem, the workpiece coordinate system $\{W\}$ relative to $\{2\}$ coordinate system can be described as Eq. (3).

$$\boldsymbol{T}_{2W} = \begin{bmatrix} c\alpha c\beta c\gamma - s\alpha s\gamma & -c\alpha s\beta s\gamma - s\alpha c\gamma & c\alpha s\beta & p_x \\ s\alpha c\beta c\gamma + c\alpha s\gamma & c\alpha c\gamma - s\alpha c\beta s\gamma & s\alpha s\beta & p_y \\ -s\beta c\gamma & s\beta s\gamma & c\beta & p_z \\ 0 & 0 & 0 & 1 \end{bmatrix} \tag{3}$$

Eq. (4) is available from Eq. (1) to Eq. (3) as below.

$$\boldsymbol{T}_{oW} = \begin{bmatrix} n_x & o_x & a_x & P_x \\ n_y & o_y & a_y & P_y \\ n_z & o_z & a_z & P_z \\ 0 & 0 & 0 & 1 \end{bmatrix} \tag{4}$$

In Eq. (4),

$$\begin{cases} n_x = c_1c_2(s\alpha s\gamma - c\alpha c\beta c\gamma) \\ \quad - c_1s_2(c\alpha s\gamma + c\beta c\gamma s\alpha) - c\gamma s\beta s_1 \\ n_y = c_2s_1(s\alpha s\gamma - c\alpha c\beta c\gamma) \\ \quad - s_1s_2(c\alpha s\gamma + c\beta c\gamma s\alpha) + c\gamma s\beta c_1 \\ n_z = s_2(c\alpha s\gamma + c\beta c\gamma s\alpha) - c_2(s\alpha s\gamma - c\alpha c\beta c\gamma) \end{cases}$$

$$\begin{cases} o_x = c_1c_2(s\alpha c\gamma + c\alpha s\beta s\gamma) \\ \quad - c_1s_2(c\alpha c\gamma - c\beta s\gamma s\alpha) + s\gamma s\beta s_1 \\ o_y = c_2s_1(c\gamma s\alpha + c\alpha s\beta s\gamma) \\ \quad - s_1s_2(c\alpha c\gamma - c\beta s\alpha s\gamma) - s\beta c_1 s\gamma \\ o_z = s_2(c\alpha c\gamma - c\beta s\alpha s\gamma) - c_2(c\gamma s\alpha + c\alpha s\beta s\gamma) \end{cases}$$

$$\begin{cases} a_x = c\beta s_1 - c\alpha s\beta c_1c_2 - s\alpha s\beta c_1s_2 \\ a_y = -c\beta c_1 - c\alpha s\beta s_2s_1 - s\alpha s\beta s_1s_2 \\ a_z = c\alpha s\beta c_2 + s\alpha s\beta s_2 \end{cases}$$

$$\begin{cases} P_x = R + s_1d_2 + p_zs_1 - p_xc_1c_2 - p_yc_1s_2 \\ P_y = -c_1d_2 - p_zc_1 - p_xc_2s_1 - p_ys_1s_2 \\ P_z = d_1 + p_xc_2 + p_ys_2 \end{cases} \tag{5}$$

In this paper, s_i is $\sin\theta_i$, c_i is the abbreviation of $\cos\theta_i$, and $s\alpha$, $s\beta$, $s\gamma$ represent $\sin\alpha$, $\sin\beta$ and $\sin\gamma$, respectively. $c\alpha$, $c\beta$, $c\gamma$ represent $\cos\alpha$, $\cos\beta$ and $\cos\gamma$, respectively.

The D-H parameters of the tool coordinate system $\{O'\}$ in Fig. 5 are shown in Table 2.

Table 2 Tool coordinate system $\{O'\}$ D-H

DOF	a_{i-1}	α_{i-1}	d_i	θ_i
O′	0	0	0	0
3	0	90	X	90
4	0	−90°	Y	−90°
5	0	−90°	Z	−90°
6	0	90°	d_6 =685	θ_3 −90°

According to the parameters of the tool coordinate system, the transformation matrix of the tool coordinate system is obtained as Eq. (6).

$$\boldsymbol{T}_{O'6} = \boldsymbol{T}_{o'3}\boldsymbol{T}_{34}\boldsymbol{T}_{45}\boldsymbol{T}_{56} = \begin{bmatrix} c_3 & -s_3 & 0 & Z \\ -s_3 & -c_3 & 0 & -Y \\ 0 & 0 & -1 & X - d_6 \\ 0 & 0 & 0 & 1 \end{bmatrix} \tag{6}$$

The polishing wheel which is processing tool is mounted on the polishing shaft on the sixth DOF of the robot.

The radius of the polishing wheel is r (150 − 300mm) and its width b is 150mm. The points on the outer circle of the polishing wheel are the processing points of the tool. The coordinates of the outer circle points of the polishing wheel are shown in Fig. 6.

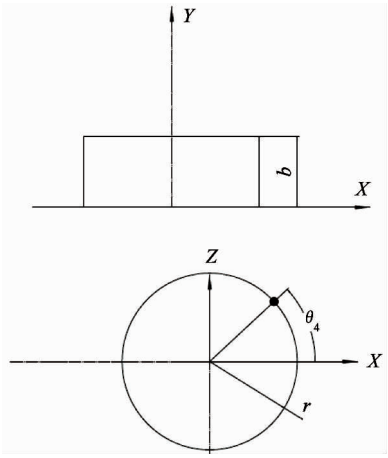

Fig. 6 The polishing wheel model

The rotation axis of the polishing wheel is Y direction of the sixth DOF. Therefore, the following Eq. (7) coordinate system is established for the outer surface of the polishing wheel.

$$\begin{cases} x = r\cos\theta_4 \\ z = r\sin\theta_4 \\ y = b \end{cases} \quad (150 \leqslant r \leqslant 300) \quad (0 \leqslant b \leqslant 150) \tag{7}$$

The outer circle surface point P of the polishing wheel is in the tool coordinate system as follows Eq. (8).

$$\boldsymbol{T}_{O'P} = \begin{bmatrix} c_3 & -s_3 & 0 & Z - bs_3 + rc_3c_4 \\ -s_3 & -c_3 & 0 & -Y - bc_3 - rc_4s_3 \\ 0 & 0 & -1 & X - d6 - rs_4 \\ 0 & 0 & 0 & 1 \end{bmatrix} \tag{8}$$

Since the X and Z axes of the O′ coordinate system are just exchanged with the O coordinate system, and the O coordinate system is in the middle, the O′ coordinate system is outside, furthermore the X and Z axes of the two coordinate systems have ΔX and ΔZ offset. So the polishing wheel relative to the fixture coordinate system is shown in the following Eq. (9).

$$\boldsymbol{T}_{OP} = \begin{bmatrix} c_3 & -s_3 & 0 & X - d6 - rs_4 + \Delta X \\ -s_3 & -c_3 & 0 & -Y - bc_3 - rc_4s_3 \\ 0 & 0 & -1 & Z - bs_3 + rc_3c_4 + \Delta Z \\ 0 & 0 & 0 & 1 \end{bmatrix} \tag{9}$$

2.2 Inverse kinematics

The polishing points of the workpiece surface are coincided with the working point of the tool coordinate system as

$$\boldsymbol{T}_{OP} = \boldsymbol{T}_{OW} \tag{10}$$

Solving this Equation, Eq. (11) is got.

$$\begin{cases} \mathrm{tg}\theta_2 = \dfrac{c\gamma s\alpha + c\alpha s\beta s\gamma}{c\alpha c\gamma - c\beta s\alpha s\gamma} \\ \mathrm{tg}\theta_1 = -\dfrac{c\alpha s\beta c_2 + s\alpha s\beta s_2}{c\beta} \\ \mathrm{tg}\theta_3 = \dfrac{c_1c_2(s\alpha c\gamma + c\alpha s\beta s\gamma)}{c_2s_1(c\gamma s\alpha + c\alpha s\beta s\gamma)} \\ s_i = \pm\sqrt{\dfrac{t_i^2}{1+t_i^2}} \\ c_i = \pm\sqrt{\dfrac{1}{t_i^2+1}} \quad (i = 1,2,3) \\ X = R + s_1d_2 + p_zs_1 - p_xc_1c_2 + d6 + rs_4 - \Delta X \\ \qquad - p_yc_1s_2 \\ Y = c_1d_2 + p_zc_1 + p_xc_2s_1 + p_ys_1s_2 - bc_3 - rc_4s_3 \\ Z = d_1 + p_xc_2 + p_ys_2 + bs_3 - rc_3c_4 - \Delta Z \end{cases} \tag{11}$$

3 Optimization of various moving DOF

3.1 Analysis on the required limit stroke of various DOF of the polishing robot

According to the analysis of previous kinematics and inverse kinematics, dimensions of the workpiece such as faucets and other bathroom parts are extended to: p_x [− 200mm, 200mm], p_y [− 200mm, 200mm], p_z [−200mm, 200mm]. The range of the workpiece attitude parameters α, β, γ is: [0, 2π], and the range of θ_4 is [0.5π, 1.5π]. The radius of the polishing wheel r is: [150mm, 300mm], the thickness of the polishing wheel b is: [0mm, 150mm].

According to these processing conditions, the required limit maximum stroke of polishing robot is analyzed to optimize the structure of polishing robot. Considering that three moving DOF of X, Y and Z is the major determinants that influent the structure compactness of the polishing robot, therefore, the limit stroke of these three DOF is analyzed in the following. According to Eq. (11), solving the limit value of X, Y, Z can be considered as an optimization problem.

There are many parameter optimization methods, such as genetic algorithm (GA), particle swarm optimization (PSO), immune optimization algorithm (IOA), simulated annealing algorithm (SAA), ant colony algorithm (ACA), neural network algorithm (NNA) and so on. The artificial fish swarm algorithm (AFSA) is used to optimize this project. The optimization method is that the maximum and minimum values of X, Y, Z are calculated, when the workpiece designated machining point is machined by applying the fish swarm algorithm, according to Eq. (11), respectively.

The flow of fish swarm algorithm is shown in Fig. 7.

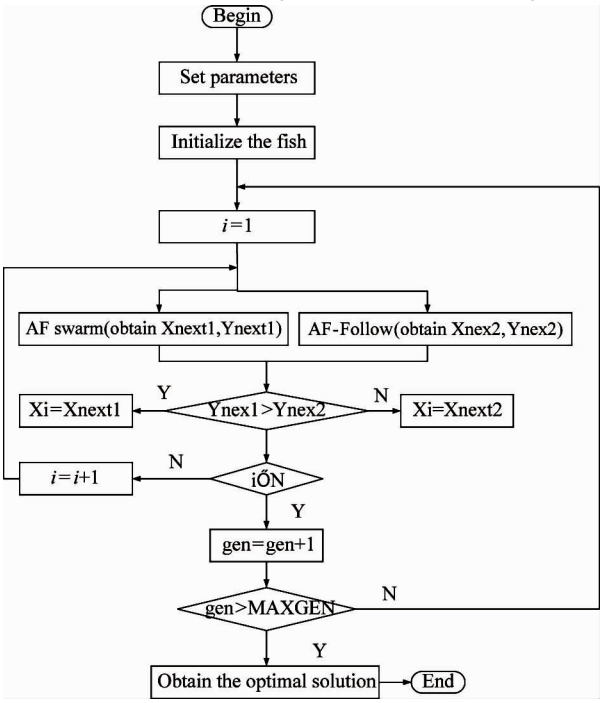

Fig. 7 The optimization of solving extreme value flow by artificial fish swarm algorithm

The parameters of artificial fish swarm algorithm are set as Table 3.

Table 3 Parameters of artificial fish swarm algorithm

item	meaning	value
fishnum	Seed number of fish sworm	1000
MAXGEN	Number of iterations	500
try _ times	Maximum foraging attempt time	500
visual	The perceived distance of artificial fish	1
Step	Moving step of artificial fish	0.1
δ	Crowded degree	0.618

Nine fish value range of this project has been mentioned above, the solution process of X, Y, Z maximum and minimum value is roughly the same, the detailed solution process of the X DOF stroke limit value is given below.

3.1.1 X maximum value solving process by artificial fish swarm algorithm

1) Parameters setting and initialization

Set parameters as Table 3, initialize the fish: α, β, γ, θ_4, P_x, P_y, P_z, r and b. Each fish range is shown in Table 4.

1000 groups of fish fry were randomly initialized within the range of Table 4.

2) Evaluation function value calculation

Calculate the value of 1000 sets of fish fry evaluation function value.

Table 4 Fish value range

fish	Minimum value	Maximum value
α	-2π	2π
β	-2π	2π
γ	-2π	2π
θ_4	0.5π	1.5π
P_x	-200	200
P_y	-200	200
P_z	-200	200
r	150	300
b	0	150

Evaluation function is

$$f_x(\alpha,\beta,\gamma,p_x,p_y,p_z,\theta 4,r,b) = R + s_1 d_2 + p_z s_1 - p_x c_1 c_2 - p_y c_1 s_2 + d_6 + r s_4 - \Delta X$$

Artificial fish swarm algorithm mainly includes foraging behavior, clustering behavior, AF-Follow behavior and random behavior.

3) Foraging behavior

Foraging behavior is the process of selecting the next state within the perceptual range, which is shown in Fig. 8.

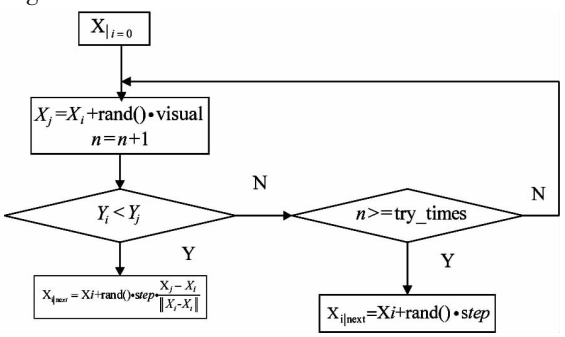

Fig. 8 The foraging behavior process

4) Clustering behavior

The clustering behavior process is shown in Fig. 9.

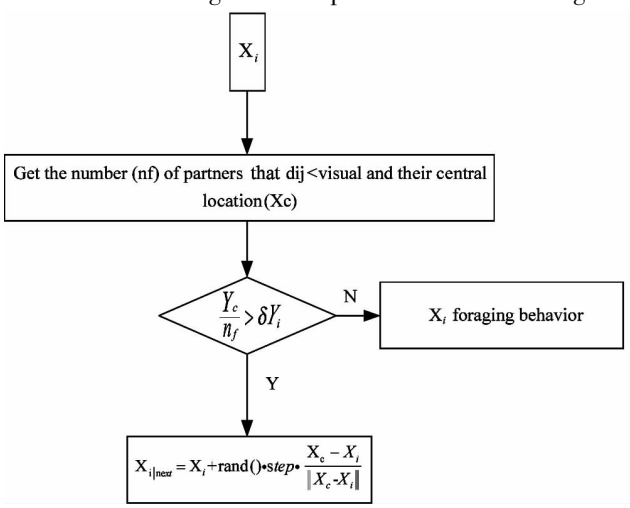

Fig. 9 The clustering behavior process

5) AF-Follow behavior

The AF-Follow behavior process is shown in Fig. 10.

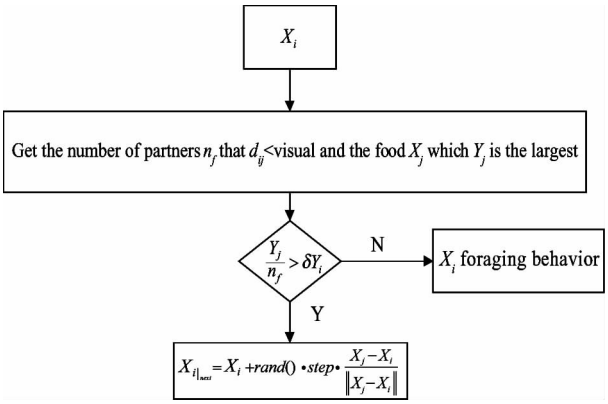

Fig. 10 The AF-Follow behavior process

6) Random behavior

The realization of random behavior is relatively simple, that is, choose a random state of vision, and then move to the state in this direction.

In fact, it is the default behavior of foraging behavior, which X_i's next position is $X_{il\ next}$

$$X_{il\ next} = X_i + r \cdot visual$$

where, r is the random number in $[-1, 1]$ interval and visual is perception distance.

After the above calculation of several algorithms, the change process of the four angle values of α、β、γ and θ_4 when solving the X maximum using artificial fish swarm algorithm is shown in Fig. 11.

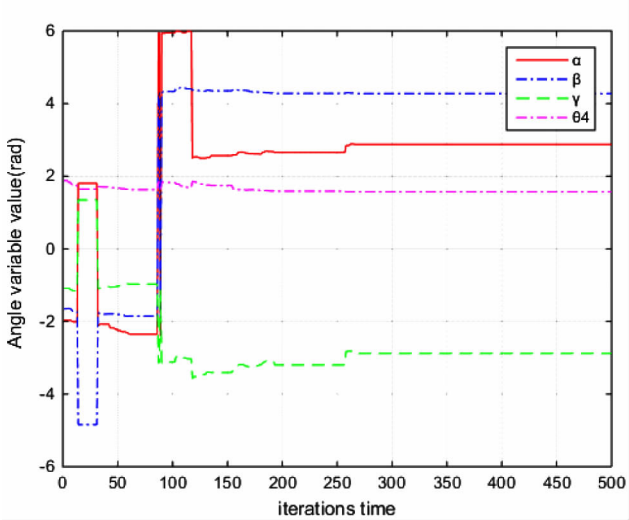

Fig. 11 The angle variable change during X maximum iteration process

The workpiece machining points (P_x, P_y, P_z) change process during the maximum X iteration process using artificial fish swarm algorithm is shown in Fig. 12.

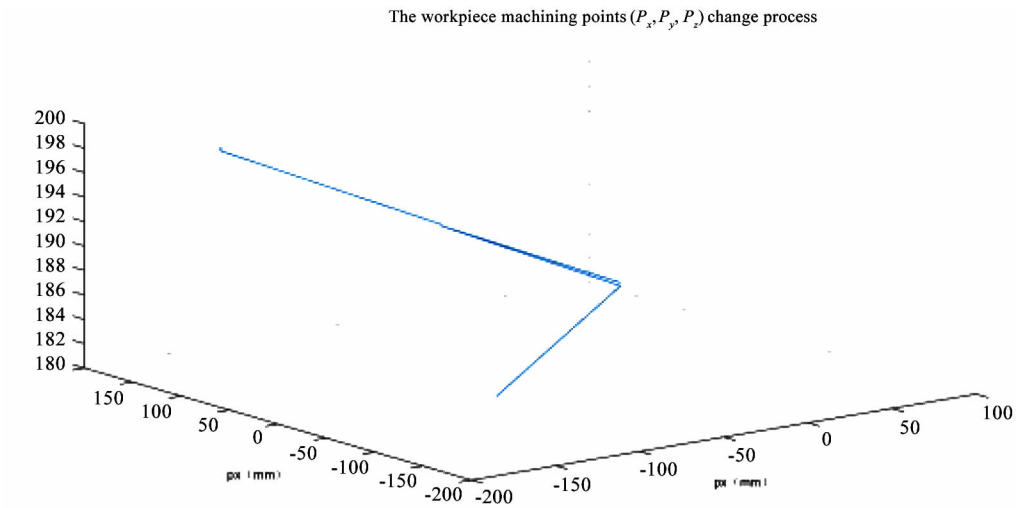

Fig. 12 The workpiece machining points (P_x, P_y, P_z) change process during the maximum X iteration process

The polish wheel parameters r and b change process during the maximum X iteration process using artificial fish swarm algorithm is shown in Fig. 13.

The maximum X iteration process is shown in Fig. 14.

The values of each variable when the X stroke is maximum are shown in Table 5.

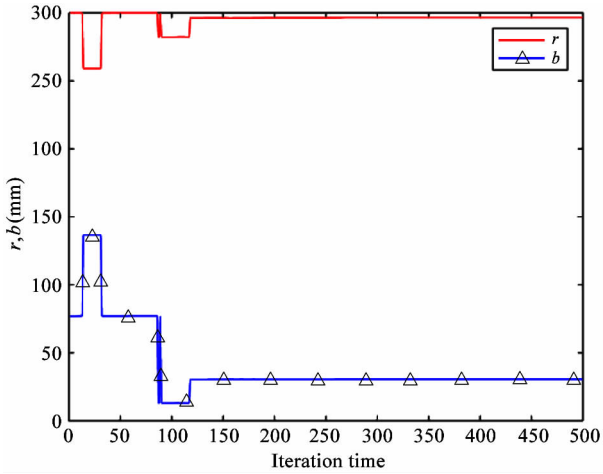

Fig. 13 The r, b change process during maximum X iteration process

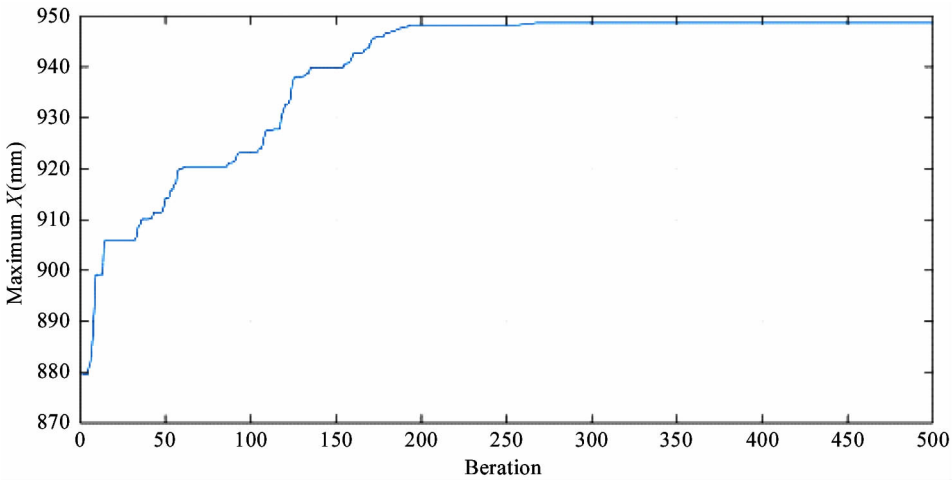

Fig. 14 The maximum X iteration process

Table 5 Each variable when X stroke is maximum

Item	Value
α (rad)	2.87663
β (rad)	4.27629
γ (rad)	-2.87778
$\theta 4$ (rad)	1.57344
P_x (mm)	-171.81685
P_y (mm)	108.07202
P_z (mm)	199.50494
r (mm)	296.66830
b	30.47379
X_{max}	948.68947

3.1.2 Various moving DOF limit stroke process result

X, Y and Z limit stroke is calculated by artificial fish swarm algorithm respectively, the optimization result is shown in Table 6.

Table 6 The stroke limit value of each DOF

Item	Value(mm)
X_{max}	948.68947
X_{min}	-469.21635
Y_{max}	700.03744
Y_{min}	-694.57027
Z_{max}	1246.40379
Z_{min}	75.04385

3.2 Dexterous polishing workspace analysis

If the robot parameters d_1, d_2, d_6, R, r, b, θ_4, $\triangle X$, $\triangle Z$ and the workpiece parameters α, β, γ, p_x, p_y, p_z are known, then the Eq. (12) about the robot unknown variables X, Y, Z, $\theta 2$, $\theta 3$ can be got according to Eq. (11).

$$\begin{cases}\theta_1 = f_1(d_1,d_2,d_6,R,r,\theta_4,\Delta X,\Delta Z,\ p_x,\ p_y,\ p_z,\alpha,\ \beta,\gamma)\\ \theta_2 = f_2(d_1,d_2,d_6,R,r,\theta_4,\Delta X,\Delta Z,\ p_x,\ p_y,\ p_z,\alpha,\ \beta,\gamma)\\ \theta_3 = f_3(d_1,d_2,d_6,R,r,\theta_4,\Delta X,\Delta Z,\ p_x,\ p_y,\ p_z,\alpha,\ \beta,\gamma)\\ X = f_4(d_1,d_2,d_6,R,r,\theta_4,\Delta X,\Delta Z,\ p_x,\ p_y,\ p_z,\alpha,\ \beta,\gamma)\\ Y = f_5(d_1,d_2,d_6,R,r,\theta_4,\Delta X,\Delta Z,\ p_x,\ p_y,\ p_z,\alpha,\ \beta,\gamma)\\ Z = f_6(d_1,d_2,d_6,R,r,\theta_4,\Delta X,\Delta Z,\ p_x,\ p_y,\ p_z,\alpha,\ \beta,\gamma)\end{cases} \tag{12}$$

The size of the workpiece to be polished in the range of (400mm × 400mm × 400mm), in order to analyze the polishing dexterity, P_x, P_y, P_Z traverse all values in the range of 400mm, and α, β, γ traverse all values in the range of $0 - 2\pi$, if the variable result value is in different DOF stroke range according to Eq. (12), this point is a dexterous processing point, and otherwise it is not the state of the dexterous processing. Define polishing robot dexterity as Eq. (13).

$$f = \frac{n}{m} \tag{13}$$

In Eq. (13), n is the total number of all dexterous processing pose points, and m is the total number of all traversal points.

Larger f means that this workpiece point can be machined with more attitude angles and more polishing wheel parameters, polishing will be more dexterous.

After analysis, all the workpiece size within (400X400X400mm) can be processed. According to the definition of dexterity Eq. (13), the dexterity of the robot is more than 0.9. If the $+ -$ sign of S_1, C_1, S_2, C_2, S_3, and C_3 in Eq. (12) are set more reasonable, the dexterity can be further improved. The analysis and calculation show that the polishing robot designed in this project has a lot of work space and has great dexterity.

3.3 Stroke optimization analysis

3.3.1 Optimized size

Considering the dimensions of faucets and other actual factors, the optimized stroke of X, Y, Z DOF is shown in Table 7.

Table 7 The optimized stroke of the polishing robot

DOF	Stroke(mm)
X	850
Y	700
Z	800

3.3.2 Verification analysis

Set $Z = 0$ and $Z = 200$ or other values to analyze the polishing dexterity of this polishing robot using above optimized XYZ stroke parameters respectively. Analysis result shows that all the points ranging in 1000mm × 1000mm on XY plane are dexterous polishing points. This processing range is much larger than the size range of our proposed workpiece, which indicates that this polishing robot can meet polishing requirement perfectly.

4 Experiment

4.1 Experiment

The multi-station rotary polishing robot at factory is shown in Fig. 15.

Fig. 15 The multi-station rotary polishing robot at factory

4.2 Machining experiment

The faucet before polishing and finished polishing is shown in Fig. 16.

(a) Before polishing (b) Finished polishing

Fig. 16 The workpiece

It can be seen that the polishing quality is high and the effect is very good.

5 Conclusion and discussion

In this paper, a novel multi-station rotary polishing robot is designed for the polishing requirement of the faucet and other bathroom parts, based on kinematics analysis, the limit stroke of XYZ DOF affecting the

compactness of robot structures is calculated by the artificial fish swarm algorithm. Considering the actual requirement, the stroke range of three moving DOF is optimized. This polishing robot has large dexterous workspace after analysis. This polishing robot can meet the polishing requirement of faucet and other bathroom parts and has more workspace allowance after simulation and machining experiment.

If this robot is only used for small-size workpiece such as faucet processing, the machine's polishing space margin is still relatively large, which can be further optimized.

In addition to the optimization of the limit stroke, the layout parameters of the robot can be further optimized, making the robot layout more reasonable.

References

[1] Mejri S, Gagnol V, Thien-Phu L, et al. Dynamic characterization of machining robot and stability analysis[J]. *International Journal of Advanced Manufacturing Technology*, 2016, 82(1-4):351-359

[2] GuoYJ, Dong H Y, Ke Y L. Oriented posture optimization in robotic machining applications[J]. *Robotics and Computer-Integrated Manufacturing*, 2015,10(35):69-76

[3] Vosniakos G, Elias M. Improving feasibility of robotic milling through robot placement optimization[J]. *Robotics and Computer-Integrated Manufacturing*, 2010, 26(5): 517-525

[4] António M L, Solteiro Pires E J. Optimization of the workpiece location in a machining robotic cell[J]. *International Journal of Advanced Robotic Systems*, 2011, 6(8): 37-46

[5] Zhang D, Yun C, Song D Z, et al. Dexterity optimization based on orthogonal test of 3P3R grinding robot[J]. *Journal of Beijing University of Aeronautics and Astronautics*, 2010, 9(36): 1075-1079(In Chinese)

[6] Zhang D . Research on Dexterity and Force Control for Robotic Polishing System: [Ph. D dissertation] [D]. Beijing: School of Mechanical Engineering and Automation, Beihang University, 2012. 25-46(In Chinese)

[7] Seriani S, Seriani M, Gallina P. Workspace optimization for a planar cable-suspended direct-driven robot [M]. London: Pergamon Press, 2015. 10-15

[8] Rao R V, Waghmare G. Design optimization of robot grippers using teaching-learning-based optimization algorithm[J]. *Advanced Robotics*, 2015, 29(6):431-447

[9] Wang X, Shi Y, Ding D, et al. Double global optimum genetic algorithm-particle swarm optimization-based welding robot path planning[J]. *Engineering Optimization*, 2016,48(2):299-316

[10] Rituparna D, Shikhar P, Bishakh B. Analysis and design optimization of a robotic gripper using multi objective genetic algorithm[J]. *IEEE Transactions on Systems, Man, and Cybernetics: Systems*, 2016, 46(1): 16-26

[11] Wang Y, Cheng L, Hou Z G, et al. Optimal formation of multi-robot systems based on a recurrent neural network [J]. *IEEE Transactions on Neural Networks and Learning Systems*, 2016, 27(2): 322-333

[12] Emine G D, Hakan G. Scheduling in two-machine robotic cells with a self-buffered robot [J]. *IIE Transactions*, 2015, 2(48): 170-191

[13] Rezaeian J B, Ghaemi O K, Ali M. Optimization of kinematic redundancy and workspace analysis of a dual-arm cam-lock robot[J]. *Robotica*, 2016, 34(1):23-42

[14] Li X L, Lu F, Tian G H, et al. Applications of artificial fish school algorithm in combinatorial optimization problems[J]. *Journal of Shandong University*, 2004, 35(5): 64-67

[15] He Q, Hu X, Ren H, et al. A novel artificial fish swarm algorithm for solving large-scale reliability-redundancy application problem[J]. *Isa Transactions*, 2015, 59:105-113

[16] Luan X Y, Li Z P, Liu T Z. A novel attribute reduction algorithm based on rough set and improved artificial fish swarm algorithm[J]. *Neurocomputing*, 2016, 174:522-529

[17] Zhang Z, Wang K, Zhu L, et al. A Pareto improved artificial fish swarm algorithm for solving a multi-objective fuzzy disassembly line balancing problem[J]. *Expert Systems with Applications*, 2017, 86:165-176

[18] Rocha A M A C, Costa M F P, Fernandes E M G P. A shifted hyperbolic augmented Lagrangian-based artificial fish two-swarm algorithm with guaranteed convergence for constrained global optimization[J]. *Engineering Optimization*, 2016, 48(12):2114-2140

[19] Yi C, Lv Y, Dang Z. A fault diagnosis scheme for rolling bearing based on particle swarm optimization in variational mode decomposition[J]. *Shock and Vibration*, 2016(2): 1-10

[20] Su J, Dong Y. Gathering the fractionated electromagnetic satellites cluster by simulating fish school[J]. *Aircraft Engineering & Aerospace Technology*, 2012, 84(2):115-119(5)

[21] Jiang H M, Xie K, Wang Y F. Optimization of pump parameters for gain flattened Raman fiber amplifiers based on artificial fish school algorithm[J]. *Optics Communications*, 2011, 284(23):5480-5483

[22] Chen G, Yin Y, Li L, et al. Mechanism and simulation of personifying intelligent decision-making for vessel collision avoidance[C] In: Proceedings of the International Conference on Computer Application and System Modeling, 2010, V4-681-V4-686

[23] Azad M A K, Rocha A M A C, Fernandes E M G P. Improved binary artificial fish swarm algorithm for the 0-1 multidimensional knapsack problems[J]. *Swarm & Evolutionary Computation*, 2014, 14:66-75

[24] Zhang Y, Guan X P. The robot path planning based on improved artificial fish swarm algorithm[J]. *Mathematical Problems in Engineering*, 2016: 1-11

[25] Duan Q, Mao M, Duan P, et al. An improved artificial fish swarm algorithm optimized by particle swarm optimization algorithm with extended memory[J]. *Kybernetes*, 2016, 45(2):210-222

[26] Li X L, Xue Y C, Lu F, et al. Parameter estimation method based-on artificial fish school algorithm[J]. *Journal of Shandong University*, 2004, 34(3):84-87(In Chinese)

Li Dongjing, born in 1978. He received his B. S. and M. S. degrees from School of Mechanical Engineering & Automation of Beihang University in 2000 and 2003, respectively. His research interests include electrical automation design, design of intelligent robot control algorithm and robot machining technology.